

Article

Long-Lived Mantle Plume and Polyphase Evolution of Palaeoproterozoic PGE Intrusions in the Fennoscandian Shield

Tamara Bayanova ^{1,*}, Aleksey Korchagin ¹, Alexander Mitrofanov ², Pavel Serov ¹, Nadezhda Ekimova ¹, Elena Nitkina ¹, Igor Kamensky ¹, Dmitry Elizarov ¹  and Milosh Huber ³

¹ Geological Institute, Kola Science Centre, Russian Academy of Sciences, 184209 Apatity, Russia; pana@geoksc.apatity.ru (A.K.); serov@geoksc.apatity.ru (P.S.); ekimova@geoksc.apatity.ru (N.E.); nitkina@geoksc.apatity.ru (E.N.); iglkam@mail.ru (I.K.); elizarov@geoksc.apatity.ru (D.E.)

² SRK Consulting, Toronto, ON M4C 1T2, Canada; mitalex1987@gmail.com

³ Department of Earth Sciences and Spatial Management, Maria Curie-Skłodowska University, 520-031 Lublin, Poland; mhuber@poczta.umcs.lublin.pl

* Correspondence: tamara@geoksc.apatity.ru; Tel.: +7-81555-7-92-18

Received: 18 October 2018; Accepted: 15 January 2019; Published: 18 January 2019



Abstract: The NE Fennoscandian Shield comprises the Northern Belt in Finland and the Southern Belt in Karelia. They host mafic-ultramafic layered Cu-Ni-Cr and Pt-Pd-bearing intrusions. Precise U-Pb and Sm-Nd analyses indicate the 130-Ma evolution of these intrusions, with major events at 2.53, 2.50, 2.45, and 2.40 Ga. Barren phases were dated at 2.53 Ga for orthopyroxenites and olivine gabbro in the Fedorovo-Pansky massif. PGE-bearing phases of gabbro-norites (Pechenga, Fedorovo-Pansky, Monchetundra massifs) and norites (Monchepluton) are 2.50 Ga old. Anorthosites of Mt. Generalskaya (Pechenga), the Fedorovo-Pansky, and Monchetundra massifs occurred at 2.45 Ga. This event produced layered PGE-bearing intrusions in Finland (Penikat, Kemi, Koitelainen) and mafic intrusions in Karelia. The Imandra lopolith dikes occurred at the final phase (2.40 Ga). Slightly negative ϵ_{Nd} and I_{Sr} values (0.703–0.704) suggest that intrusions originated from an enriched mantle reservoir. Low $^3\text{He}/^4\text{He}$ ratios in accessory minerals (ilmenite and magnetite) indicate an upper mantle source. Large-scale correlations link the Fennoscandian Shield with the Superior and Wyoming cratons.

Keywords: Plume; LIP; PGE; Palaeoproterozoic; mafic intrusion; U-Pb; isotopes

1. Introduction

The NE Fennoscandian (Baltic) Shield covers the Archaean crust formed at 3.5–2.7 Ga [1,2]. The post-Archaean evolution is mainly reflected in rifting and emplacement of mafic-ultramafic complexes along NE-trending structures. The NE Baltic Shield hosts the Southern (Fenno-Karelian) Belt (FKB) and the Northern (Kola) Belt (KB) that we studied in detail in our profound research [3].

FKB extends 350 km along the northern edge of the Karelian craton. It comprises Palaeoproterozoic mafic-ultramafic layered bodies in Finland (e.g., Penikat, Kemi) [4–6], Sweden (Tornio intrusion), and Russia (Olanga group) [7] that occurred in similar geodynamic settings [8].

KB strikes northwestwards for over 500 km. It borders the SW edge of the Archaean Kola-Norwegian Block and the Northern and Southern edges of the Palaeoproterozoic Pechenga-Imandra-Varzuga rift. There are several layered mafic-ultramafic bodies [7]. Layered PGE-bearing pyroxenite-norite-gabbro-anorthosite intrusions occur at the boundaries between early Proterozoic rifts lying over the Archaean basement [9,10].

The purpose of this work is a complex study of Palaeoproterozoic Pt-Pd and Cu-Ni intrusions that are widespread in the NE Baltic Shield. We use a set of isotope techniques to define precision ages

of formation of reefs, lower and upper parts of layered intrusions, host rocks, and cutting dyke series. We also aimed at studying sources of primary magmas and primary reservoirs. The main objective of this research is to compare new isotope data with those on other Palaeoproterozoic intrusions of the Finnish group, Northern America, and Canada. This would corroborate the model of the plume mantle source for all Palaeoproterozoic intrusions.

The current study continues our investigations [3], but substantiates it with new isotope geochronological data. It allowed us to define that PGE-bearing intrusions of the Fennoscandian Shield referred to the enriched mantle reservoir EM-1. This paper provides new data showing that magmatism in the Kola-Karelian Province correlates with the peak of mafic-ultramafic magmatism in the Superior and Wyoming provinces (2.45 Ga).

2. Geological Setting

The Palaeoproterozoic East Scandinavian Large Igneous Province (LIP) occurs in the NE Fennoscandian Shield (Figure 1). Its granulite and gneiss-migmatite basement originated at >2550 Ma. This province had several stages of magmatism and sedimentation separated by breaks (conglomerates). The Sumian stage (2550–2400 Ma) was crucial for the production of Pt-Pd ores [9,10]. In FKB, the magmatism was most active at 2450 to 2400 Ma [4,10–16]. In KB, PGE-bearing intrusions formed at 2530–2450 Ma.

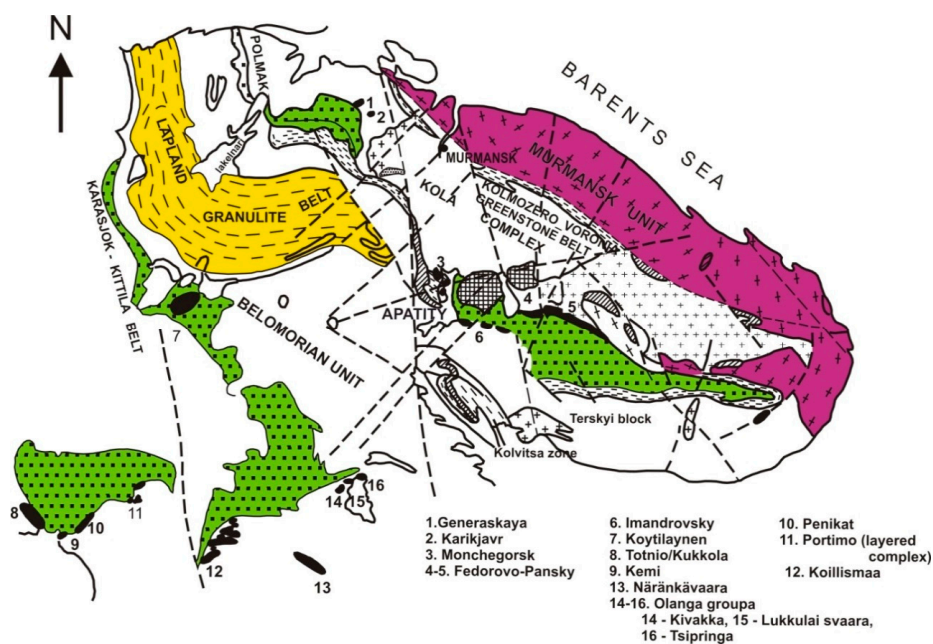


Figure 1. Sketch map of the Palaeoproterozoic East Scandinavian LIP in the Northern Fennoscandian Shield [15].

The Fedorovo-Pansky Layered Complex strikes north-westwards for >60 km and dips Southwestwards at an angle of 30–35° (Figure 2). The Fedorov, Lastjavr, Western and Eastern Pansky are its major blocks [9]. This complex is bordered by the Archaean Keivy terrain and the Palaeoproterozoic Imandra-Varzuga rift. In the North, the complex borders alkaline granites of the White Tundra intrusion. Their U-Pb age on zircon is 2654 + 15 Ma [17]. The contact of the Western Pansky Block with the Imandra-Varzuga volcano-sedimentary sequence mostly has Quaternary deposits. However, drill and excavation works to the South of Mt. Kamennik reveal a strongly sheared and metamorphosed contact between the intrusion and overlying Palaeoproterozoic volcano-sedimentary rocks.

The authors had earlier studied the Fedorovo-Pansky massif using a full set of geological, mineralogical, petrographical, and geochemical methods [3]. This allowed us to identify the block structure of the massif and define zones with different composition, age, and mineralization. Provided below is a compilation of previously obtained data [3] and results of this study.

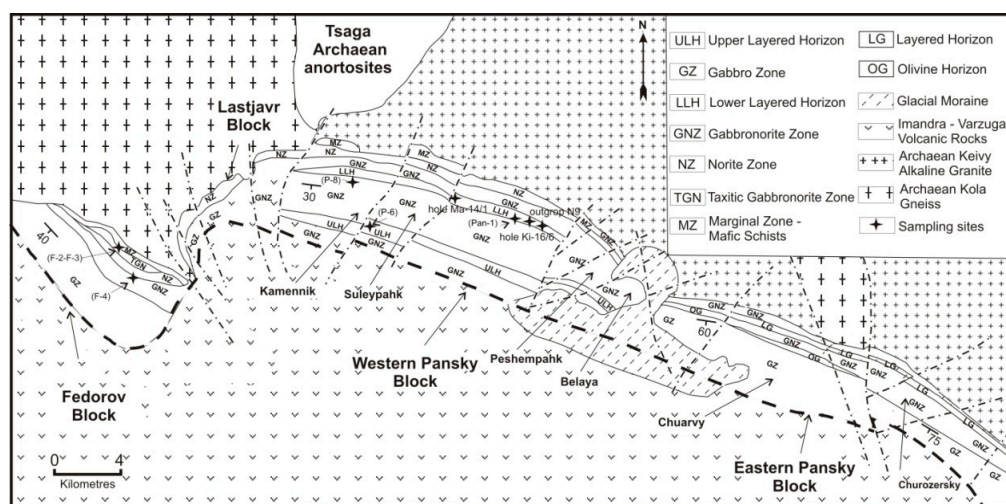


Figure 2. Sketch geological map of the Fedorovo-Pansky massif [9].

The Fedorovo-Pansky Complex consists of Marginal, Taxitic, and Norite zones (Figure 2). The Marginal Zone contains plagioclase-amphibole schists, massive fine-grained norites, and gabbronorites. The Taxitic Zone contains ore-bearing gabbronorites (2485 Ma), xenoliths of plagioclase-bearing pyroxenite and norite (2526–2516 Ma), syngenetic and magmatic ores (Pt and Pd sulfides, Cu and Ni sulfides with Pt, Pd and Au, bismuth-tellurides and arsenides). The Norite Zone hosts harzburgite and plagioclase-bearing pyroxenite with Cu-Ni-PGE mineralization in the lower part. These rocks are chromium-rich (up to 1000 ppm) and contain chromite. The same mineralization occur in FKB intrusions [5].

The Fedorov Block is a part of the Fedorovo-Pansky Complex. The Layered Lower Horizon (LLH) of its Main Gabbronorite Zone is composed of gabbronorite, norite, pyroxenite and interlayers of leucocratic gabbro and anorthosite, and reef-type PGE deposit. The Upper Layered Horizon (ULH) consists of olivine-bearing troctolite, norite, gabbronorite, and anorthosite. It comprises several layers of PGE-rich ore (Pd > Pt) [9]. The U-Pb age of the ULH rocks on single-grain zircon and baddeleyite is 2447 ± 12 Ma. This age shows that ULH rocks are the youngest in the Fedorovo-Pansky Complex.

The Fedorov Tundra Block is in the West of the Fedorovo-Pansky massif. It contains mafic and rare ultramafic rocks, mostly gabbronorites with highly heterogeneous mineral grains. The contact-type Cu, Ni, and PGE mineralization is economically valuable.

There are three mineral types of the sulfide mineralization: pyrrhotite, pyrrhotite-chalcopyrite, and pentlandite-chalcopyrite-pyrrhotite. The latter type is best-valued commercially, since it contains the complex PGE mineralization.

Major ore minerals are chalcopyrite, pyrrhotite and pentlandite. Their average proportions recalculated for 100% sulfide are 41%, 35%, and 24%, respectively. In the total amount of sulfides, their portion is 95–100%. Secondary and accessory minerals are pyrite, ilmenite, magnetite, mackinawite, marcasite, cubanite, millerite, bornite, sphalerite, and violarite.

Besides pentlandite, chalcopyrite and pyrrhotite may also host minor PGE, though lower than pentlandite [18], i.e., kotulskite, merenskyite, braggite, stillwaterite, vysotskite, and sobolevskite for palladium; braggite, moncheite, merenskyite, and sperrylite for platinum; and gold-silver alloys for gold [19,20]. In total, 29 PGE and gold minerals, as well as eight PGE phases with no status of individual minerals, have been recorded in the ore. Microprobe analyses of their chemical compositions have been conducted in the Geological Institute KSC RAS [20,21].

3. Materials and Methods

U-Pb (TIMS) Method with $^{208}\text{Pb}/^{235}\text{U}$ Tracer [12,22–25], Zircon ID-TIMS U-Pb Analyses (with a ^{205}Pb Spike) [12,24,25], ID-TIMS Sm-Nd Analyses of Silicates [12,22,23,26,27], ID-TIMS Rb-Sr

Analyses [12,28], ID-TIMS Sm-Nd Analyses of Sulfides [12,13,23,24,26,29–31], Electron Microprobe and LA-ICP-MS Major and Trace Element Analyses [32] have been used to study the samples.

3.1. Isotope Analyses

The U-Pb concordia plot and Sm-Nd isochron methods are applied to define the age of crystallization of the rocks. U-Pb zircon and baddeleyite ages for the same sample are commonly coherent. They indicate a similar age of the magma crystallization and subsequent transformations. Coordinates of baddeleyites are near the concordia line. However, it is difficult to apply this method due to minor amounts of zircon and baddeleyite grains in these rocks.

Compared to the precise U-Pb systematics with an error of ca. 0.1%, the Sm-Nd method is not an accurate geochronometer (error of ca. 2–3%). However, it allows defining the crystallization age of mafic rocks using major rock-forming minerals. The method is especially important for dating rocks with syngenetic ore minerals. It has been used to date (2482 ± 36 Ma) the early gabbro and second anorthosite (2467 ± 39 Ma) ore bodies in the Fedorovo-Pansky deposit. This deposit is considered to be economically important [33].

Sm-Nd ages of the KB mafic-ultramafic intrusions overlap because of large errors. The estimations are compatible with U-Pb ages obtained on zircon and baddeleyite. They are especially important for marginal fast-crystallizing rocks of the Taxitic Zone within the Fedorovo-Pansky Complex. The ages of early barren orthopyroxenite and gabbro are 2521 ± 42 Ma and 2516 ± 35 Ma (Sm-Nd method) and 2526 ± 6 Ma and 2516 ± 7 Ma (U-Pb method). The ore-bearing norite of the Fedorov Block yields ages of 2482 ± 36 Ma (Sm-Nd method) and 2485 ± 9 Ma (U-Pb method) [34,35].

Importantly, the Sm-Nd method provides valuable petrological and geochemical markers, i.e., $\epsilon\text{Nd}(T)$ and TDM. The ϵNd value shows a degree of the mantle source depletion, while TDM indicates an approximate age of melt extraction from the mantle protolith [35].

The Rb-Sr whole-rock and mineral-isochron method, specific trace elements (Cu, Ni, Ti, V, and LREE), ϵNd (2.5 Ga) and $^4\text{He}/^3\text{He}$ data, values of initial $^{87}\text{Sr}/^{86}\text{Sr}$ ($I_{\text{Sr}}[2.5 \text{ Ga}]$) indicate an enriched 2.5 Ga-old mantle reservoir [36]. It is similar with the modern EM-I reservoir [37,38] and corroborated by the Re-Os systematics [39].

3.2. LA-ICP-MS

The distribution of rare and precious metals in sulfide parageneses has been first studied in detail using the laser ablation inductively coupled plasma mass spectrometry (LA-ICP-MS). It enables detecting regular patterns of the element distribution with a high degree of accuracy. The results indicate that pentlandite in sulfide parageneses of the Fedorov Tundra deposit has commercially valuable PGE mineralization.

The method of LA-ICP-MS (UP-213 laser, high-resolution Element-XR mass spectrometer with ionization) has been applied to analyze concentrations of Cr, Co, As, Se, Ru, Rh, Pd, Ag, Cd, Sb, Re, Os, Ir, Pt, Au, Tl, Pb, and Bi in sulfides. The following parameters have been accepted for the analysis: crater diameter is 40 μm , impulse frequency of laser radiation is 4 Hz. The samples have been analyzed by blocks, which were prepared using the Element XR software. Standard samples have been measured at the beginning and end of each block. Internal laboratory sulfide standards have been used for analysis. The deviation by calibration standards is 10–20%. Fe has been applied, having quite high concentrations in relation to background values. It occurs in all of the studied samples and is the most homogeneously distributed in phases.

Regional PGE-bearing deposits are represented by the basal and reef-like types. According to modern economic evaluation, the basal type is preferable for mining, even if the PGE content (1–3 ppm) is lower than in reef-type deposits (>5 ppm). Basal deposits are thicker and contain more Pt, Cu, and especially, Ni.

In the Eastern Fennoscandian Shield, the Palaeoproterozoic magmatic activity is associated with the formation of Cu-Ni (\pm PGE), Pt-Pd (Rh, \pm Cu, Ni, Au), Cr, and Ti-V deposits [40,41]. The Fedorov deposit is best-valued for PGE (Pt, Pd, Rh), but Ni, Cu, and Au are also economically

important [10]. Ore-forming magmatic and post-magmatic processes are closely related to the Taitic Zone gabbronorite of the 2485 ± 9 Ma magmatic pulse. Reef-type deposits (Pt-Pd (\pm Cu, Ni, Rh, Au) and ore occurrences of the Western Pansky Block (Fedorovo-Pansky Complex) are genetically associated with pegmatoid leucogabbro and anorthosite rich in late-stage fluids. Portions of this magma produce additional injections of ca. 2500 Ma, ca. 2470 Ma (the Lower, Northern PGE reef) and ca. 2450 Ma (the Upper, Southern PGE reef of the Western Pansky Block and PGE-bearing mineralization of Mt. General'skaya intrusion). These magma injections are quite similar in their prevalence of Pd over Pt, ore mineral composition [9] and isotope geochemistry of the Sm-Nd and Rb-Sr systems. ϵ Nd values for these rocks vary from -2.1 to -2.3 . This may indicate a single long-lived enriched magmatic source.

High contents of Cr (>1000 ppm) are typical of lower mafic-ultramafic rocks from layered intrusions in the Baltic Shield [4,5]. The chromite mineralization occurs in basal series of the Monchepluton, Fedorovo-Pansky Complex, Imandra lopolith (Russia), Penikat [42] and Narkaus intrusions (Finland), chromite deposits of the Kemi intrusion (Finland) [43] and Dunite Block (Monchepluton, Russia). In contrast, the Fe-Ti-V mineralization of the Mustavaara intrusion (Finland) tends to occur in the leucocratic-most parts of layered series, as well as in leucogabbro-anorthosite and gabbro-diorite of the Imandra lopolith (Russia) and Koillismaa Complex (Finland).

4. Results

4.1. Fedorovo-Pansky Massif: U-Pb and Sm-Nd Isotope Data

Several large samples have been selected in the Fedorovo-Pansky Complex for further isotope analyses. Medium- and coarse-grained gabbronorite have been sampled in LLH of the Eastern Kievev area. Three types of zircons (transparent, with a vitreous luster) have been separated [3]: Pan-1, regular bipyramidal-prismatic crystals of up to $120 \mu\text{m}$; Pan-2, fragments of prismatic crystals; and Pan-3, pyramidal apices of crystals of $80\text{--}100 \mu\text{m}$. In immersion view, all the zircons display a simple structure with fine zoning and cross jointing.

The previously obtained data show that the crystallization time of the main gabbronorite phase of LLH is 2491 ± 1.5 Ma, since the upper intersection age is 2491 ± 1.5 Ma (MSWD = 0.05) and the lower intersection is at zero and indicates the loss of Pb (Figure 3a, Table 1) [3,7,44]. The same zircon sample has been analyzed at the Royal Ontario Museum laboratory (Canada). It proved slightly older (2501.5 ± 1.7 Ma) [45].

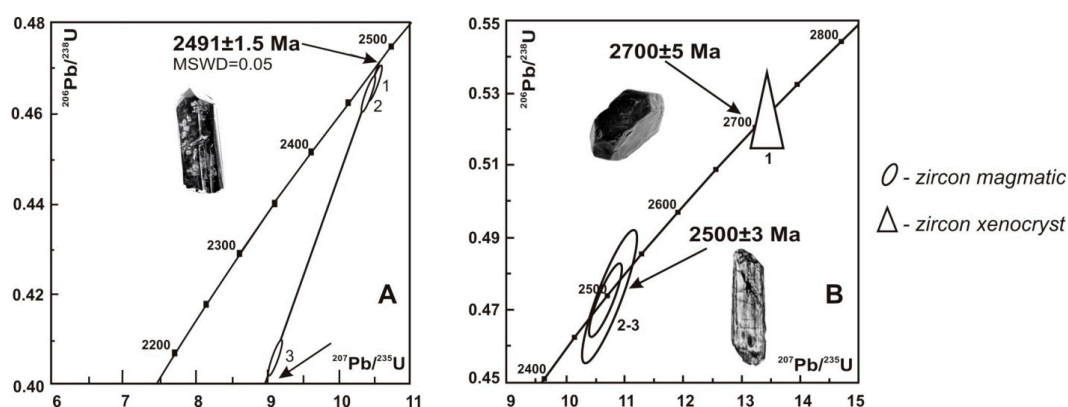


Figure 3. (a) Isotope U-Pb concordia diagrams for magmatic zircon (2-3) and (b) zircon xenocryst (1) from gabbronorite of the Western-Pansky Block of the Fedorovo-Pansky massif.

Table 1. Isotope U-Pb data on baddeleyite (Bd) and zircon (Zr) on the Western-Pansky and Fedorov Blocks of the Fedorovo-Pansky massif.

Sample No	Weight (mg)	Content (ppm)		Pb Isotope Composition ¹			Isotope Ratios ²		Age ² (Ma)
		Pb	U	$\frac{206\text{Pb}}{204\text{Pb}}$	$\frac{206\text{Pb}}{207\text{Pb}}$	$\frac{206\text{Pb}}{208\text{Pb}}$	$\frac{207\text{Pb}}{235\text{U}}$	$\frac{206\text{Pb}}{238\text{U}}$	$\frac{207\text{Pb}}{206\text{Pb}}$
Western-Pansky Block, gabbro-norites (Pan-1)									
1	3.30	95.0	144	11740	6.091	3.551	10.510	0.4666	2491
2	1.60	84.0	144	6720	6.062	3.552	10.473	0.4650	2491
3	1.90	70.0	142	10300	6.100	4.220	9.135	0.4061	2489
Western-Pansky Block, gabbropegmatite (P-8)									
1	5.90	95.0	158	3240	5.991	3.081	10.435	0.4681	2471
2	7.30	181.0	287	8870	6.161	2.260	10.092	0.4554	2465
3	1.25	125.0	200	3400	6.012	2.312	10.082	0.4532	2468
Western-Pansky Block, anorthosite (P-6)									
1	0.75	218.0	322	5740	6.230	3.263	11.682	0.5352	2438
2	0.10	743.0	1331	3960	6.191	3.151	9.588	0.4393	2438
3	0.20	286.0	577	2980	6.021	3.192	8.643	0.3874	2474
4 (bd)	1.00	176.0	396	14780	6.290	63.610	9.548	0.4380	2435
5(bd)	0.26	259.0	560	3360	6.132	54.950	9.956	0.4533	2443
Fedorov Block, orthopyroxenite (F-3)									
1	0.75	48.0	60.9	825	4.9191	1.3039	10.0461	0.44249	2504
2	0.80	374.0	598.6	4588	6.0459	1.9650	9.6782	0.43153	2484
3	0.85	410.2	630.2	4521	6.0281	1.6592	9.5667	0.42539	2488
4	1.00	271.0	373.1	2552	5.9916	1.2393	9.4700	0.42406	2476
Fedorov Block, olivine gabbro (F-4)									
1	1.80	725.3	1322.8	14649	6.1121	3.8177	10.0132	0.44622	2484
2	2.00	731.3	1382.8	8781	6.1522	3.5517	9.4306	0.42454	2467
3	1.95	680.9	1374.0	7155	6.2645	3.6939	8.7401	0.40155	2433
Fedorov Block, PGE-bearing gabbro-norite (F-2)									
1	0.30	498.0	833.4	2081	5.9502	2.2111	9.49201	0.42493	2477
2	0.65	513.8	932.2	5274	6.1519	2.6371	9.1373	0.41378	2458
3	0.55	583.2	999.3	3194	6.1132	2.0528	8.9869	0.40832	2452
4	0.80	622.5	1134.5	4114	6.1161	2.1914	8.6638	0.39165	2460

¹ All ratios are corrected for blanks of 0.1 ng for Pb and 0.04 ng for U, mass discrimination $0.17 \pm 0.05\%$. ² Correction for common Pb has been determined for the age according to [25].

In the framework of this research, the authors have conducted new measurements using single zircon grains from the main PGE gabbro-norite phase from the old collection (Figure 3b, Table 2) and obtained the similar age of 2500 ± 3 Ma. The isotope Sm-Nd data show the age of the same gabbro-norite on the main rock-forming minerals and whole-rock is 2487 ± 51 Ma (MSWD = 1.5) [16].

Table 2. U-Pb data on single zircon xenocryst (1) and magmatic zircon (2,3) from gabbronorite of the Fedorovo-Pansky massif.

No.	Weight mg	Content (ppm)			Isotope Composition ¹			Isotope Ratios and Age in Ma ²			% Dis
		Pb	U	²⁰⁶ Pb/ ²⁰⁴ Pb	²⁰⁶ Pb/ ²³⁸ U ± 2σ	²⁰⁷ Pb/ ²³⁵ U ± 2σ	²⁰⁷ Pb/ ²⁰⁶ Pb ± 2σ	²⁰⁶ Pb/ ²³⁸ U ± 2σ	²⁰⁷ Pb/ ²³⁵ U ± 2σ	²⁰⁷ Pb/ ²⁰⁶ Pb ± 2σ	
1	0.0457	21.20	6.33	833.59	0.521 ± 0.018	13.327 ± 0.634	0.186 ± 0.006	2702 ± 95	2703 ± 129	2704 ± 82	0.1
2	0.0536	12.87	5.92	461.17	0.474 ± 0.015	10.768 ± 0.393	0.165 ± 0.003	2499 ± 80	2503 ± 91	2507 ± 42	0.3
3	0.0567	16.10	10.96	111.20	0.472 ± 0.008	10.688 ± 0.215	0.164 ± 0.002	2495 ± 42	2496 ± 50	2498 ± 26	0.1

¹ Ratios are corrected for blanks of 1 pg for Pb and 10 pg for U, mass discrimination 0.12 ± 0.04%. ² Correction for common Pb has been determined for the age according to Reference [25].

In contrast with the zircon age, the rock-forming minerals originate at the post-magmatic stage. However, considering measurement errors, Sm-Nd ages are suggested to be close to the U-Pb ones.

Three types of zircon have been extracted from PGE-bearing gabbro-pegmatite (LLH). Zircons from samples P-8, D-15 and D-18 have been used for isotope analyses [3]. The concordant U-Pb age on zircons from PGE-bearing gabbro-pegmatite (LLH) is 2470 ± 9 Ma (MSWD = 0.37) (Figure 3a, Table 1). The lower intersection of the discordia line (c. 300 Ma) indicates a loss of Pb. This indicates the Palaeozoic tectonic activity in the Eastern Baltic Shield [3,46].

Analyses of whole-rock and rock-forming silicate and sulfide minerals from gabbro pegmatite give a Sm-Nd age of 2467 ± 39 Ma, MSWD = 1.8. εNd(T) is negative with -1.4 ± 0.5 (Figure 4a, Table 3). Noteworthy, these ages are quite similar within the measurement error.

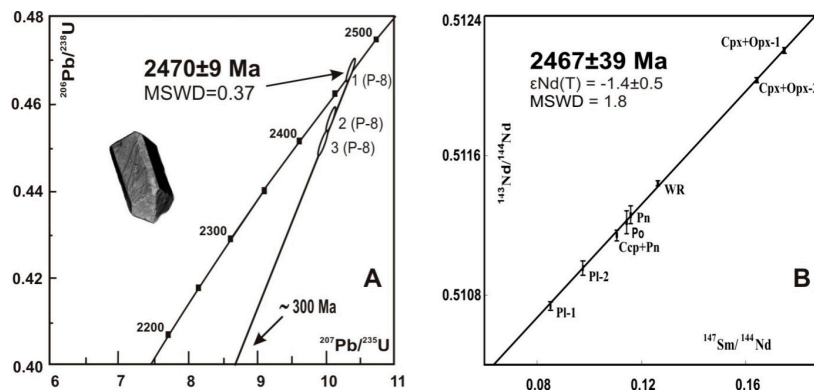


Figure 4. Isotope U-Pb diagram on zircon (a) and Sm-Nd mineral isochron for rock-forming and sulfides minerals (b) from gabbronorite (LLH) of the Fedorovo-Pansky massif.

Table 3. Sm-Nd data on rock-forming and sulfide minerals from gabbronorite (LLH) of the Fedorovo-Pansky massif.

Sample No.	Content, ppm		Isotope Ratios		T _{DM} , Ma	ε _{Nd} (T)
	Sm	Nd	¹⁴⁷ Sm/ ¹⁴⁴ Nd	¹⁴³ Nd/ ¹⁴⁴ Nd		
Gabbro-pegmatite LLH						
WR	1.038	4.99	0.1263	0.511441 ± 10	2967	-1.3
Po	0.033	0.147	0.1144	0.511217 ± 69		
Pn	0.011	0.041	0.1160	0.511259 ± 53		
Pl-1	0.332	2.30	0.0853	0.510738 ± 24		
Pl-2	0.398	2.25	0.0977	0.510957 ± 39		
Cpx + Opx-1	4.75	16.44	0.1747	0.512209 ± 7		
Cpx + Opx-2	2.54	9.34	0.1641	0.512033 ± 9		
Ccp + Pn	0.022	0.124	0.1106	0.511143 ± 27		

Average standard values during measurements: N = 11 (La Jolla: = 0.511833 ± 10); N = 100 (JNdi1: = 0.512098 ± 15).

The U-Pb age is identical to the Sm-Nd one. Hence, we can suggest a very narrow closure temperature in the U-Pb (zircon) and Sm-Nd (rock-forming and sulfide minerals) systematics.

Three types of zircon and two varieties of baddeleyite (Sample P6-1) have been separated in ULH of the Southern Suleypahk area. The authors had previously studied and described zircons from samples Pb-1, Pb-2 and Pb-3 [3]. The U-Pb results for these samples define a discordia line intersecting the concordia curve at 2447 ± 12 Ma, MSWD = 2.7 (Figure 5a, Table 1). This age indicates the origin of late phase anorthosite, since baddeleyite forms mainly in residual igneous melts [3,47].

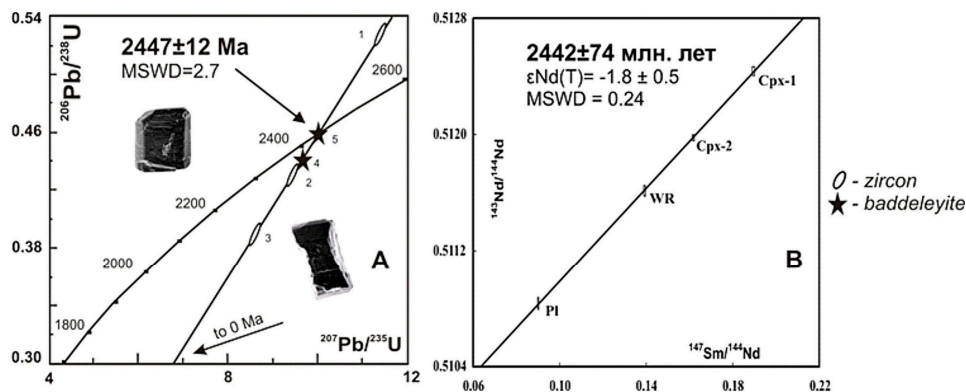


Figure 5. Isotope U-Pb age (a) on baddeleyite (4-5) and zircon (1-2-3); Sm-Nd mineral isochron (b) for rock-forming minerals and WR from anorthosites in ULH of the Fedorovo-Pansky massif.

A similar age is obtained from Sm-Nd data on rock-forming minerals of ULH anorthosite, i.e., 2442 ± 74 Ma with slightly negative $\epsilon_{Nd}(T) = -1.8 \pm 0.5$, MSWD = 0.24 (Figure 5b, Table 4).

Table 4. Sm-Nd data on whole rock and rock-forming minerals from ULH anorthosite of the Fedorovo-Pansky massif.

Sample No.	Content, ppm		Isotope Ratios		T_{DM} , Ma	$\epsilon_{Nd}(T)$
	Sm	Nd	$^{147}\text{Sm}/^{144}\text{Nd}$	$^{143}\text{Nd}/^{144}\text{Nd}$		
ULH anorthosite						
WR	0.271	1.176	0.1393	0.511613 ± 34	3131	-0.8
Pl	0.107	0.719	0.0901	0.510833 ± 39		
Cpx-1	0.921	2.94	0.1896	0.512436 ± 32		
Cpx-2	0.801	2.99	0.1618	0.511978 ± 20		

Average standard values during measurements: $N = 7$ (La Jolla: $= 0.511837 \pm 8$); and $N = 32$ (JNdi1: $= 0.512097 \pm 19$).

The U-Pb zircon age of early barren orthopyroxenite (F-3) from the Fedorov Block (2526 ± 6 Ma) marks the emplacement time (Figure 6a, Table 1). The similar U-Pb age (Figure 6b, Table 1) has also been obtained using zircon from barren olivine gabbro (F-4). Cu-Ni-PGE-bearing taxitic gabbro (F-2) from the Fedorov Block (Figure 6c, Table 1) yield a U-Pb age on zircon of 2485 ± 9 Ma [34].

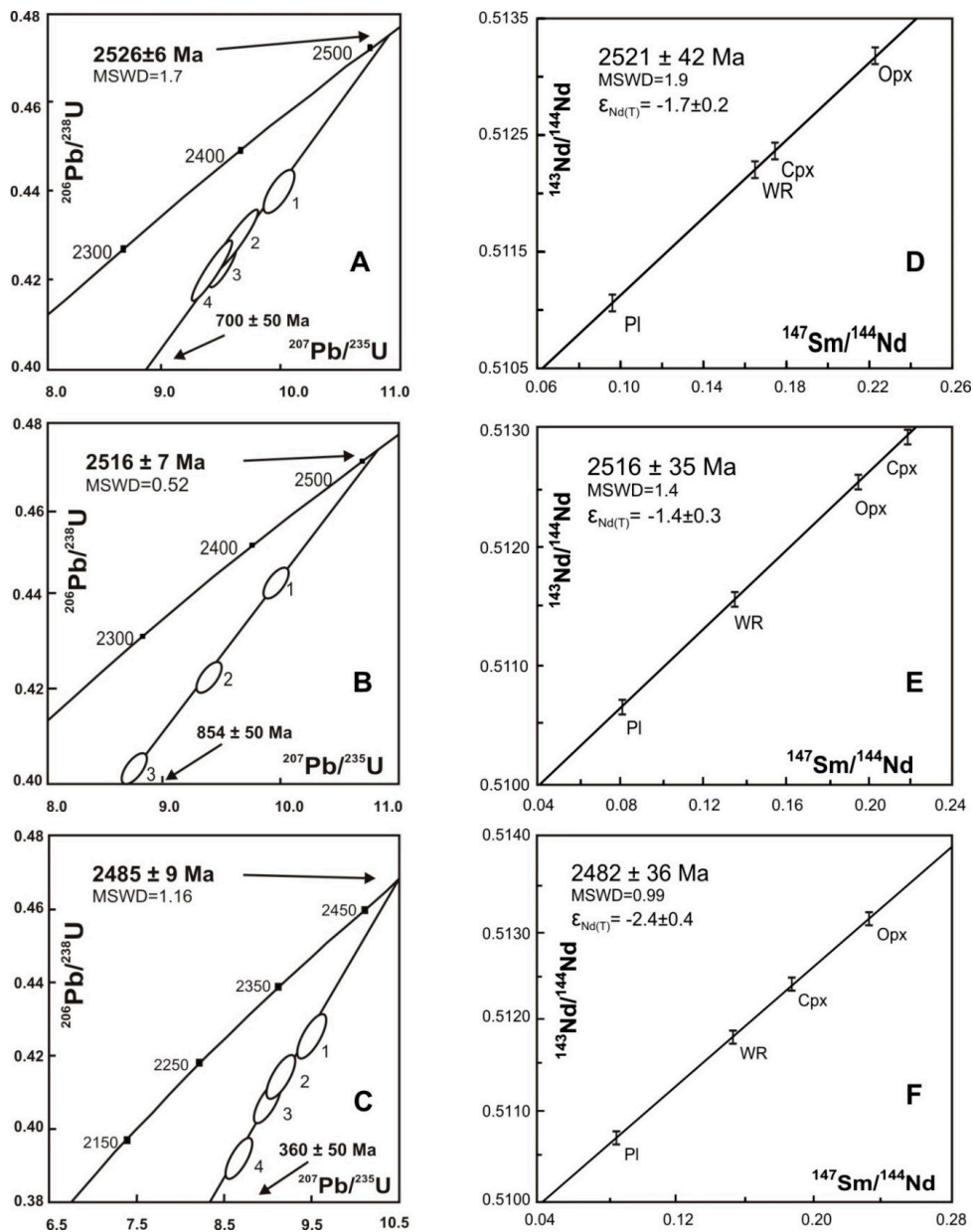


Figure 6. Isotope U-Pb ages on zircon (A–C) and Sm-Nd isochrones (D–F) for rock-forming minerals from the Fedorov Block of the Fedorovo-Pansky massif.

Isotope analyses of these samples using the whole rock, pyroxene and plagioclase yield ages that correspond to the respective U-Pb ages on zircon (Figure 6d–f). Table 5 provides a compilation of the previously obtained results [3] and new results of isotope geochemical research.

Table 5. Sm-Nd data on whole rock and rock-forming minerals from the Fedorov Block of the Fedorovo-Pansky massif.

Sample No.	Content (ppm)		Isotope Ratios		T_{DM} (Ga)	Sm-Nd (Ma)	ϵ_{Nd} (2.5Ga)
	Sm	Nd	$^{147}\text{Sm}/^{144}\text{Nd}$	$^{143}\text{Nd}/^{144}\text{Nd}$			
D-orthopyroxenite (F-3)							
WR	0.32	1.17	0.1648	0.512196 ± 12	3.05	2521 ± 42	-1.73
Opx	0.12	0.38	0.2228	0.513182 ± 16			
Cpx	2.21	7.67	0.1745	0.512349 ± 17			
Pl	0.26	1.62	0.0960	0.511071 ± 29			
E-olivine gabbro (F-4)							
WR	0.63	2.80	0.1357	0.511548 ± 8	2.94	2516 ± 35	-1.53
Opx	0.23	0.72	0.1951	0.512555 ± 15			
Cpx	0.83	2.28	0.2187	0.512947 ± 16			
Pl	0.24	1.77	0.0815	0.510677 ± 14			
F-PGE-bearing gabbro (F-2)							
WR	0.42	1.66	0.1537	0.511807 ± 20	3.18	2482 ± 36	-2.50
Pl	0.41	2.88	0.0865	0.510709 ± 14			
Cpx	1.78	5.73	0.1876	0.512387 ± 8			
Opx	0.13	0.33	0.2323	0.513088 ± 40			

Average standard values during measurements: N = 10 (La Jolla: = 0.511835 ± 11); and N = 22 (JNdil: = 0.512097 ± 16).

4.2. Fedorovo Tundra Deposit: Trace Element Compositions

Three samples from different areas of the Fedorovo Tundra deposit have been investigated: sample BGF-237-132 from olivine-bearing gabbro of the Bolshoy Ikhtegipakhk, samples BGF-487-50.5 and BGF-495-76.5 from gabbro of the Pakhkaraka area.

Mantle normalized diagrams (Figures 7 and 8, Table 6) show ratios of the obtained contents for each measured component normalized to the primitive mantle. Dashed areas indicate dispersion of the obtained results.

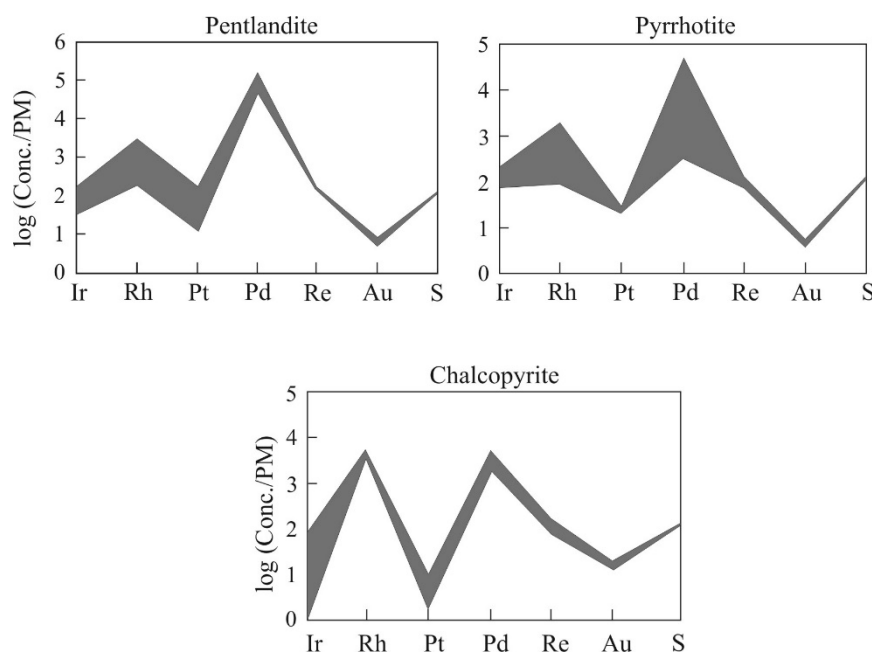


Figure 7. Mantle normalized diagram showing the distribution of PGEs, Au, and Re in sulfides (composition of the primitive mantle is according to Reference [48]).

Table 6. Contents (ppm) of different elements in sulfide parageneses of the Fedorovo Tundra deposit.

Sample	Mineral	Number of Analyses	Cr	Co	As	Se	Ru	Rh	Pd	Ag	Cd	Sb	Re	Os	Ir	Pt	Au	Tl	Pb	Bi
237/132.0	Pentlandite	8	2.8–16.5	6811–10681	0.3–0.7	92–183	0.5–1.0	0.1–6.9	258–1221	0.4–5.8	-	0.1–0.1	-	0.1	0.01–0.2	0.01–1.2	0.01	0.1–0.8	0.2–8.1	0.02–0.2
	Chalcopyrite	6	2.8	0.3–142	0.3	178	0.2	0.1–9.1	19	0.2–5.3	14	0.1–0.2	0.02	0.1	0.3	0.01	0.03	-	4.5–8.0	-
487/50.5	Pentlandite	10	0.9–5.9	8395	0.3–0.4	99	0.8	1.5–9.1	442	0.7	-	0.1	0.05	0.1–0.3	0.6	0.03–0.2	-	0.1–0.4	0.1–2.3	0.02
	Pyrrhotite	8	0.6–453	59–15612	0.2–2.5	102–222	0.3–1.5	1.2–2.9	0.1–636	0.1–1.6	-	0.1	0.03–0.09	0.2–0.6	0.6–1.1	0.2	0.01	0.1–1.4	0.1–5.8	0.01–0.04
495/76.5	Chalcopyrite	5	-	-	0.5–0.7	98	0.2	8.8	18	0.4	5	0.1	-	-	-	-	-	-	1.5	-
	Pentlandite	10	2.0	5499–12079	0.4	118	0.6–1.2	0.1–0.6	247–1487	0.3–1	-	0.1	-	0.2	0.3	0.2–2	0.01	0.1–0.9	0.1–1.5	0.03–0.1
	Pyrrhotite	9	0.7–15	66–119	-	132	0.2	0.1–0.2	0.1–4	0.4–2	-	0.1	0.03	0.1	0.1–0.3	0.04–0.3	0.01	0.02–0.05	0.1–6.3	0.02–0.6
	Chalcopyrite	8	2.6	0.5–487	0.7	142	0.1–0.2	11	23–125	0.6–1133	2–9	-	0.04	-	0.02	0.02–0.1	0.02	0.04–0.7	0.6–4.1	0.04–0.2

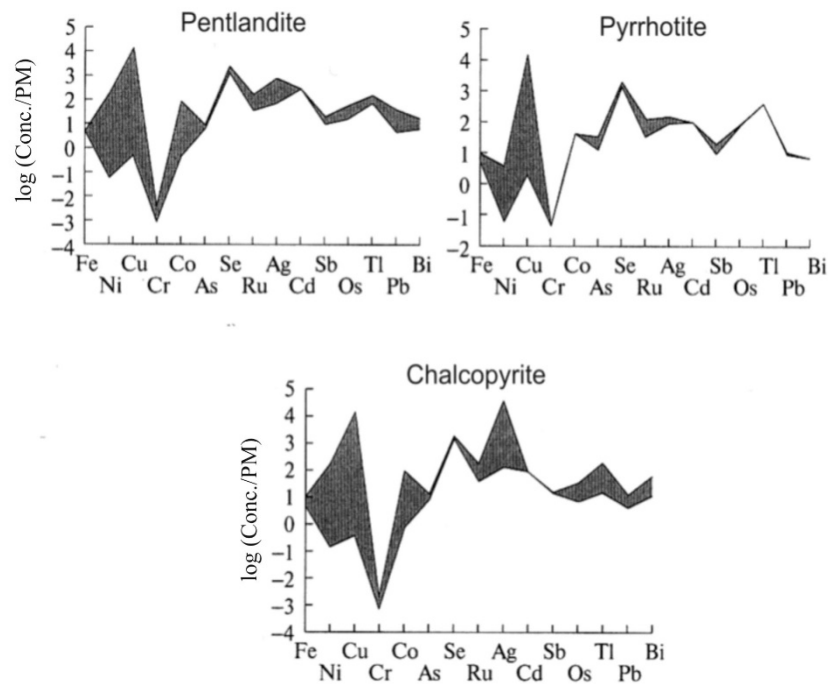


Figure 8. Mantle normalized diagram showing the distribution of some trace elements in sulfides (composition of the primitive mantle is according to References [49,50]).

Pentlandite is the main concentrator of Co and PGEs (Pd, Ru, and Pt). Since Pt and Pd are the best-valued commercial minerals of the Fedorovo Tundra deposit, pentlandite can be considered the most important among economic sulfide minerals of this deposit, along with PGMs. However, the abundance of pentlandite is much higher.

Pyrrhotite has a significant content of Cr and PGEs (Ir and Os). Pyrrhotite is the major concentrator of As and Bi.

Chalcopyrite accumulates almost all Ag and a significant proportion of Au. This mineral has high contents of Pb and Rh either.

Se, Re, Sn, and Ta are quite homogeneously distributed in all of the three mineral phases.

4.3. Penikat (Sompujarvi reef) and Kemi Intrusions: Sm-Nd and U-Pb Geochronology

Gabbro-norites (about 30 kg) were sampled in a geological field trip headed by M. Iljina (Geological Survey of Finland) to the Penikat and Kemi intrusions in 2008. The concordant age on 2 types of zircon from gabbro-norite is 2430 ± 2 Ma. The concordant age on three types of zircon from the Kemi sample is 2447 ± 4 Ma (Figure 9b,c, Table 7).

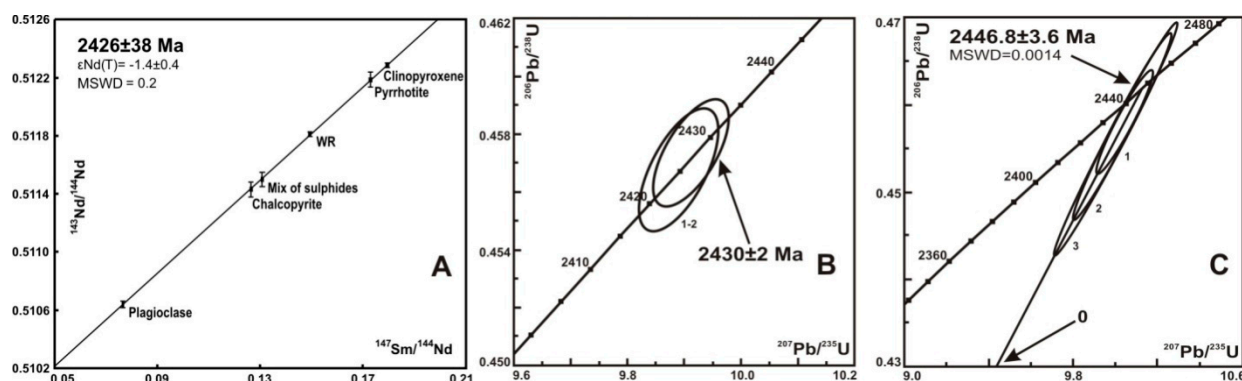


Figure 9. Mineral Sm-Nd isochron for PGE-bearing gabbronorites (a), the U-Pb age on single zircon (b) from the Penikat intrusion and the U-Pb age on single zircon grains (c) from the Kemi intrusion (Finland), FKB.

Table 7. U-Pb data on single zircon from layered PGE intrusions in Finland.

No.	Weight mg	Content (ppm)		Isotope Composition ¹			Isotope Ratios and Age in Ma ²			% Dis	
		Pb	U	$^{206}\text{Pb}/^{204}\text{Pb}$	$^{206}\text{Pb}/^{238}\text{U} \pm 2\sigma$	$^{207}\text{Pb}/^{235}\text{U} \pm 2\sigma$	$^{207}\text{Pb}/^{206}\text{Pb} \pm 2\sigma$	$^{206}\text{Pb}/^{238}\text{U} \pm 2\sigma$	$^{207}\text{Pb}/^{235}\text{U} \pm 2\sigma$		$^{207}\text{Pb}/^{206}\text{Pb} \pm 2\sigma$
Gabbronorite of Penikat											
1	0.1360	24.87	33.26	260.12	0.458 ± 0.004	9.929 ± 0.138	0.157 ± 0.002	2429 ± 21	2428 ± 34	2428 ± 24	-0.04
2	0.1840	28.14	42.74	254.48	0.457 ± 0.004	9.845 ± 0.138	0.156 ± 0.002	2426 ± 21	2420 ± 34	2416 ± 24	-0.41
Gabbronorite of Kemi											
1	0.027	13.84	18.52	358.23	0.463 ± 0.009	10.155 ± 0.205	0.1592 ± 0.0005	2452 ± 49	2449 ± 49	2447 ± 7	-0.2
2	0.057	13.61	19.18	758.23	0.459 ± 0.009	10.069 ± 0.202	0.1592 ± 0.0005	2434 ± 48	2441 ± 49	2447 ± 7	0.5
3	0.032	11.51	16.10	404.27	0.453 ± 0.009	9.948 ± 0.196	0.1592 ± 0.0005	2410 ± 47	2430 ± 48	2447 ± 7	1.3

¹ Ratios are corrected for blanks of 1 pg for Pb and 10 pg for U, mass discrimination of $0.12 \pm 0.04\%$. ² Correction for common Pb has been determined for the age according to Reference [25].

The Sm-Nd isotope ages of rock-forming and sulfide minerals are much coeval to the U-Pb zircon data that suggested a very narrow closure temperature at the time of origination.

The whole rock, silicates and sulfides of the Penikat intrusion have a Sm-Nd age of 2426 ± 38 Ma (MSWD = 0.2) (Figure 9a, Table 8). It agrees with the Sm-Nd age of 2410 ± 64 Ma determined for the Penikat intrusion earlier [51]. Importantly, sulfide data lie on the isochron as well. It testifies to the coincidence of sulfide formation and the rock crystallization. Table 9 provides compiled isotope data obtained in previous [3] and the current research.

Table 8. Sm-Nd data on whole rock, rock-forming and sulfide minerals from ore-bearing gabbronorite of the Penikat layered intrusion.

	Content, ppm		Isotope Ratios			Model Age, Ma		ϵ_{Nd}
	Sm	Nd	$^{147}\text{Sm}/^{144}\text{Nd}$	$^{143}\text{Nd}/^{144}\text{Nd}$	Err.	CHUR	DM	
WR	2.004	10.066	0.14938	0.511811	28	2655	3155	-1.4
Plagioclase	0.654	3.655	0.07654	0.510639	22			
Clinopyroxene	1.901	6.398	0.17956	0.512285	9			
Chalcopyrite	0.109	0.647	0.13085	0.511499	53			
Pyrrhotite	0.301	2.017	0.17299	0.512185	47			
Sulfide mix	0.114	0.709	0.12648	0.511431	46			

Average standard values during measurements: N =7 (La Jolla: = 0.511836 ± 12); N = 21 (JNdi1: = 0.512097 ± 15).

Table 9. Sm-Nd and Rb-Sr data on whole rock from layered Palaeoproterozoic complexes of the Fennoscandian Shield.

Sample No.	Content (ppm)		Isotopic Ratios		ϵ_{Nd} (2.5 Ga)	T_{DM} (Ga)	$^{87}Rb/^{86}Sr$	$^{87}Sr/^{86}Sr (\pm 2\sigma)$, 2.5 Ga
	Sm	Nd	$^{147}Sm/^{144}Nd$	$^{143}Nd/^{144}Nd (\pm 2\sigma)$				
Fedorovo-Pansky intrusion								
Pan-1, gabbro	0.762	3.293	0.139980	0.511669 \pm 7	−2.00	2.98	0.00135	0.7032 \pm 1
Pan-2, gabbro	0.423	1.662	0.153714	0.511807 \pm 20	−2.50	3.18	0.00174	0.7029 \pm 2
F-4, olivine gabbro	0.629	2.801	0.135695	0.511548 \pm 8	−1.53	2.94	0.00144	0.7029 \pm 2
F-3, orthopyroxenite	0.318	1.166	0.164803	0.512196 \pm 12	−1.73	3.05	0.00205	0.7033 \pm 2
Monchetundra								
MT-10, medium-grained pyroxenite	0.483	1.913	0.152689	0.511925 \pm 33	−0.36	2.81	0.00495	0.7039 \pm 2
Mt. Generalskaya								
S-3464, gabbro	1.147	5.362	0.129320	0.511449 \pm 14	−2.30	2.91	0.00534	0.7042 \pm 2
Imandra lopolith								
6-57, gabbro	2.156	10.910	0.119130	0.511380 \pm 3	−2.00	2.88	0.00339	0.7046 \pm 3
Penikat								
gabbro	2.004	10.066	0.149380	0.511810 \pm 15	−1.40	3.16	0.00527	0.7039 \pm 5
Kemi								
gabbro	0.532	3.162	0.134950	0.511821 \pm 9	−1.90	2.98	0.00431	0.7041 \pm 8
Monchepluton								
M-1, quartz norite	1.750	8.040	0.131957	0.511493 \pm 3	−1.51	2.91	0.01053	0.7034 \pm 9
H-7, gabbro	0.920	4.150	0.134055	0.511537 \pm 4	−1.37	2.90	0.00227	0.7037 \pm 2

5. Discussion

A full set of advanced isotope geochronological methods has been applied to study the largest and ore-richest deposits of the Fedorovo-Pansky Complex. Table 10 is a data base of U-Pb and Sm-Nd ages of PGE layered intrusions in the Fennoscandian Shield. It includes both available and new data obtained by the authors of this study.

Previously, the authors had suggested that these PGE intrusions occurred at the same interval [3]. Based on U-Pb and Sm-Nd data, the authors defined zones with different ages in the Fedorov Block, Western Pansky Block of the Fedorovo-Pansky Complex, Monchetundra massif, Mt. Generalskaya and Imandra lopolith [3]. This study corroborates and substantiates results of the previous research. New data prove that, in the suggested hypothesis, there were four pulses of the magmatic activity associated with the formation of PGE intrusions of the Fennoscandian Shield in the interval 2.53–2.40 Ga.

The Fedorov Block of the Fedorovo-Pansky Complex represents an independent magma chamber. Its rocks and ores differ significantly from those of the Western Pansky Block [3,10]. A 2 km-thick rock sequence stretches from as a layered or differentiated syngenetic series. The age of melanocratic pyroxenite-norite-gabbro between the Marginal Zone to the Lower Gabbro Zone is 2526 ± 6 and 2516 ± 7 Ma. The Taxitic Zone is intruded by concordant Cu-Ni-PGE-bearing gabbro (Fedorov deposit) of the second-pulse magmatic injection (2485 ± 9 Ma).

Table 10. U-Pb and Sm-Nd data on PGE layered intrusions of the Fennoscandian Shield.

Layered Intrusions	Age (Ma)		$\epsilon_{Nd(T)}^2$ U/Pb age	
	U-Pb	Sm-Nd		
KB				
Mt. Generalskaya				
Gabbronorite	2496 ± 10 ¹ (2505 ± 1.6) ²	2453 ± 42 ¹	−2.3	
Anorthosite	2446 ± 10 ¹			
Monchepluton				
Dunite block, dike	2505 ± 1.7 ¹⁹			
Mt. Travyanaya, norite	2507 ± 9 ¹⁵			
Dunite block, gabbronorite dike	2506 ± 10 ¹⁵ ; 2496 ± 14 ¹⁵			
Nyud Terrace, gabbronorite	2500 ± 5 ¹⁴			
Nyud Terrace, gabbronorite	2493 ± 7 ¹ (2504 ± 1.5) ²	2492 ± 31 ³	−1.4	
Nyud Terrace, gabbronorite	2503.5 ± 4.6 ¹⁹			
Monchepluton, gabbronorite	2498.2 ± 6.7 ¹⁹			
Vurechuaivench foothills, metagabbronorite	2497 ± 21 ¹⁵ ; 2498.2 ± 6.7 ¹⁷			
Olenegorsk deposit, quartz diorite, dike	2495 ± 13 ¹⁵			
Main Ridge				
Monchetundra, plagiopyroxenite	2502.3 ± 5.9 ¹⁶			
Monchetundra, gabbronorite	2504 ± 7.4 ¹⁶			
Monchetundra, gabbro	2463 ± 25 ⁴ ; 2453 ± 4 ⁵			
Monchetundra, gabbronorite	2501 ± 8 ¹⁴ ; 2505 ± 6 ¹⁴			
Monchetundra, gabbropegmatite	2445.1 ± 1.7 ¹⁶			
Chunatundra, anorthosite	2467 ± 7 ¹⁵			
Ostrovsky intrusion, gabbronorite-pegmatite	2445 ± 11 ¹⁵			
Fedorovo-Pansky massif				
Orthopyroxenite	2526 ± 6 ¹²	2521 ± 42 ¹³	−1.7	
olivine gabbro	2516 ± 7 ¹²	2516 ± 35 ¹³	−1.4	
magnetite gabbro	2498 ± 5 ⁶ ; 2500 ± 10 ¹⁶			
Gabbronorite	2491 ± 1.5 ⁷ (2501 ± 1.7) ²	2487 ± 51 ⁷	−2.1	
	2500 ± 3 ¹⁹			
Cu-Ni PGE-bearing gabbronorite	2485 ± 9 ¹² ; 2500 ± 3 ²¹	2482 ± 36 ¹³	−2.4	
PGE-gabbropegmatite	2470 ± 9 ⁷	2467 ± 39 ²¹	−1.4	
PGE-anorthosite	2447 ± 12 ⁷	2442 ± 74 ²¹	−1.8	
Imandra lopolith				
Gabbronorite	2446 ± 39 ⁷ (2441 ± 1.6) ²	2444 ± 77 ⁷	−2.0	
gabbrodiorite-pegmatite	2440 ± 4 ⁶			
Norite	2437 ± 7 ⁶			
leucogabbro-anorthosite	2437 ± 11 ⁶			
Granophyre	2434 ± 15 ⁶			
olivine gabbronorite (dike)	2395 ± 5 ⁶			
monzodiorite dike	2398 ± 21 ⁶			
FKB				
Kivakka, olivine gabbronorite	2445 ± 2 ⁷	2439 ± 29 ⁸	−1.2	
Lukkulaisvaara, pyroxenite	2439 ± 11 ⁷ (2442 ± 1.9) ²	2388 ± 59 ⁸	−2.4	
Tsipringa, gabbro	2441 ± 1.2 ²	2430 ± 26 ⁸	−1.1	
Burakovskaya intrusion, gabbronorite	2449 ± 1.1 ²	2365 ± 90 ⁸	−2.0	
Aganozero body		2372 ± 22 ²⁰	−3.2	
Shalozero-Burakovo Intrusive Body		2433 ± 28 ²⁰	−3.1	
Kovdozero intrusion, pegmatoid gabbronorite	2436 ± 9 ⁶			
FINNINIS GROUP				
Koitelainen	2433 ± 8 ⁹	2437 ± 49 ¹¹	−2.0	
Koilismaa	2436 ± 5 ¹⁰			
Nyaryankavaara	2440 ± 16 ¹⁰			
Penikat	2430 ± 2 ²¹	2410 ± 64 ⁹ ; 2426 ± 38 ¹⁸	−1.6; −1.4	
Akanvaara	2437 ± 7 ¹¹	2423 ± 49 ¹¹	−2.1	
Kemi	2446.8 ± 3.6 ²¹			
¹ [52]	⁵ [55]	⁹ [57]	¹³ [35]	¹⁷ [62] ¹⁸ [33] ¹⁹ [63] ²⁰ [64] ²¹ Present study
² [45]	⁶ [56]	¹⁰ [58]	¹⁴ [60]	
³ [53]	⁷ [16]	¹¹ [59]	¹⁵ [12]	
⁴ [54]	⁸ [56]	¹² [34]	¹⁶ [61]	
			¹⁷ [62]	

The Western Pansky Block in the Main Gabbronorite Zone, excluding LLH and probably the upper part (above 3000 m), is a single syngenetic series of relatively leucocratic, mainly olivine-free gabbronorite-gabbro. They crystallized at 2526–2485 Ma. The Norite and Marginal Zones occur in the lower part of the Block. The Marginal Zone contains the poor disseminated Cu-Ni-PGE mineralization.

This rock series can be correlated with certain parts of the Fedorov Block. LLH is 40–80 m-thick. It has a unique structure with dominant leucocratic anorthositic rocks. The exposed part of the horizon strikes for almost 15 km and can be traced in boreholes down to a depth of 500 m [8]. Morphologically, the horizon seems to be a part of a single layered series. Nevertheless, there are anorthositic bodies with cross-cutting contacts and apophyses in outcrops [19]. Cumulus plagioclase compositions of the rocks in the horizon are different from those in surrounding rocks. The age of PGE-bearing leucogabbro-pegmatite (2470 ± 9 Ma) is precisely defined by concordant and near-concordant U-Pb data on zircon. It is slightly younger than ages of surrounding rocks (e.g., 2491 ± 1.5 Ma and 2500 ± 3 Ma). The LLH rocks, especially the anorthosite and PGE mineralization, are likely to represent an independent magmatic pulse.

The upper part and olivine-bearing rocks of the Western Pansky Block differ from the main layered units of the Block in rock, mineral and PGE mineralization composition [9]. Up to date, only one reliable U-Pb age (2447 ± 12 Ma) has been obtained for PGE-bearing anorthosite in the block. New Sm-Nd estimates yield an age of 2467 ± 39 Ma, which is much coeval to the U-Pb data.

The early magmatic activity at ca. 2.5 Ga reflects in gabbro-norites of the Monchetundra (2505 ± 6 and 2501 ± 8 Ma) and Mt. General'skaya (2496 ± 10 Ma). The magmatic activity that produced anorthosite took place at ca. 2470 and 2450 Ma. It also contributed to a layered series of the Chunutundra (2467 ± 7 Ma) and Mt. General'skaya (2446 ± 10 Ma), Monchetundra gabbro (2453 ± 4 Ma) and pegmatoid gabbro-norite of the Ostrovsky intrusion (2445 ± 11 Ma) (Table 10) [12].

The Imandra lopolith is the youngest large layered intrusion in KB. It differs from other KB intrusions both in its emplacement age and metallogeny. There are five U-Pb zircon and baddeleyite ages for the rocks of the main magmatic pulse. They were formed at 2445–2434 Ma.

Thus, several intrusions have been established in KB, including at least four intrusions (or phases) in the Fedorovo-Pansky Complex: a 2526–2516 Ma barren intrusion and three ore-bearing ones of 2505–2485, 2470, and 2450 Ma. For similar intrusions of FKB, e.g., the Penikat intrusion in Finland, five intrusions varying in geochemistry only have been distinguished from the same deep chamber [5].

A total duration for magmatic processes of over 130 Ma in the KB intrusions is surprising. The multi-phase magmatic duration of the FKB intrusions was short-term and took place about 2.44 Ga years ago. However, there are only a few U-Pb precise age estimations for the FKB intrusions [5]. Results for the Kola prove that layering of the intrusions with thinly-differentiated horizons and PGE reefs was not contemporaneous (or syngenetic). It was defined that each intrusion has its own metallogenic trend in time and space.

The magmatic activity revealed from 2.53 to 2.40 Ga with intrusions at 2.53, 2.50, 2.45, and 2.40 Ga. These four intrusions are based on precise U-Pb ages on single zircon and baddeleyite grains. The first three intrusions are corroborated by the Sm-Nd mineral isochron ages within the measurement error.

Since the Palaeoproterozoic (2.53 Ga), magmatic processes have affected most of the Kola-Lapland-Karelian province, after the continental crust became mature by ca. 2.55 Ga in the Neoarchean [65]. Here, up to 3 km-thick basaltic volcanites of the Sumian age (2.53–2.40 Ga) cover an area of more than 200 000 km². In the north, magmatic analogues of these volcanic rocks are represented by two belts of layered intrusions and numerous dike swarms [14,66,67]. These units have similar geological, compositional and metallogenic features [68]. Jointly, they compose the East-Scandinavian LIP. Its geological settings indicate anorogenic rift-like intraplate arrangements. They link volcano-plutonic belts connecting different domains of the Palaeoarchean Kola-Lapland-Karelia protocontinent. This resembles the early advection extensional geodynamics of passive rifting that is typical of intraplate plume processes [69,70]. Geochemical and isotope-geochemical data (ϵ Nd values -1.1 to -2.4 , I_{Sr} values 0.703–0.704) indicate the single homogenous mantle source of the LIP rocks (Figure 10). This mantle source was enriched with both siderophile and lithophile elements, including LREE. This reservoir resembles the modern EM-1 source [37,38].

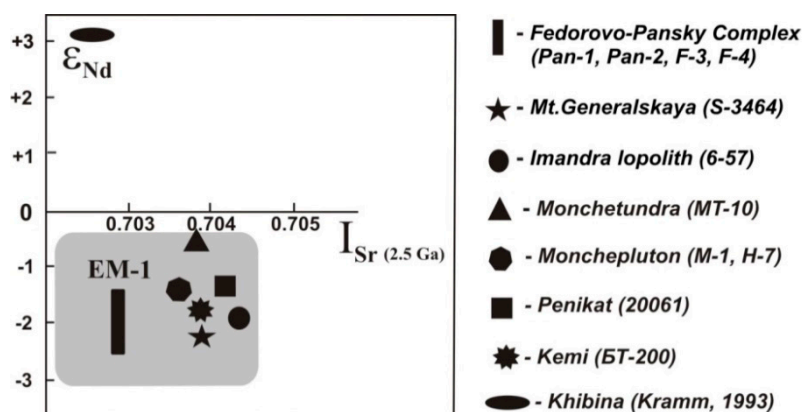


Figure 10. Plot of ϵ_{Nd} - I_{Sr} for the KB and FKB layered intrusions. Grey color indicates an EM-1 reservoir at the time of the layered intrusions formation. Sm-Nd and Rb-Sr isotope data are provided in Table 9.

Isotope $^4\text{He}/^3\text{He}$ ratios are another reliable isotope tracer of mantle plume processes [56,70,71]. Their use in the Precambrian study requires further consideration. He isotope data on rocks and minerals of the KB intrusions show that the $^4\text{He}/^3\text{He}$ isotope ratios of $n \times 10^6$ and $n \times 10^5$ correspond to ratios of the upper mantle and differ from those of the crust ($n \times 10^8$) and lower mantle ($n \times 10^4$) [3, 12,71]. According to these data, crustal contamination was local.

The LIP layered intrusions are directly related to the Fennoscandian Shield metallogeny [39]. The evolution of the two belts of layered mafic complex (2.53 to 2.40 Ga) encompasses a group of younger (2.44 Ga) intrusions within FKB [5,72].

The peak of the mafic-ultramafic magmatic activity in the Kola-Karelian, Superior and Wyoming provinces was at ca. 2.45 Ga (Figure 11) [3,12,67,69,72–74]. This study proves that layered intrusions in KB and FKB (2.53–2.40 Ga) had an intraplate nature. The Kola is considered as a part of the “greater” Karelia craton (Figure 11).

We consider a LIP as a product of a vast long-lived plume, according to geochemical data (Table 10). The studied East-Scandinavian LIP, or mafic LIP, has the following features:

- gravity anomalies caused by a crust-mantle layer at the bottom of the crust;
- riftogenic (anorogenic) structural ensembles with multipath extensional fault tectonics identified by the distribution of grabens and volcanic belts, dike swarms, and intrusive belts;
- protracted polyphase tectonics and magmatism, continental discontinuities and erosion with early stages of tholeiitic-basalt (trappean), boninite-like, and subalkaline magmatism in the continental crust, possible closing stages of the Red Sea-type spreading magmatism;
- intrusive sills, lopoliths, sheet-like bodies, large dikes and dike swarms. The intrusions are often layered and differ from rocks formed in subduction and spreading zones, with trends of thin differentiation layering, limited development of intermediate and felsic rocks, often with leucogabbro and anorthosite ends and abundant pegmatoid mafic varieties;
- typical mantle geochemistry of rocks and ores, as registered by isotope mantle tracers: $^{143}\text{Nd}/^{144}\text{Nd}$, $^{87}\text{Sr}/^{86}\text{Sr}$, $^{187}\text{Os}/^{188}\text{Os}$, and $^3\text{He}/^4\text{He}$;
- large orthomagmatic Cr, Ni, Cu, Co, PGE ($\pm\text{Au}$), Ti, and V deposits [18,69,72,75,76].

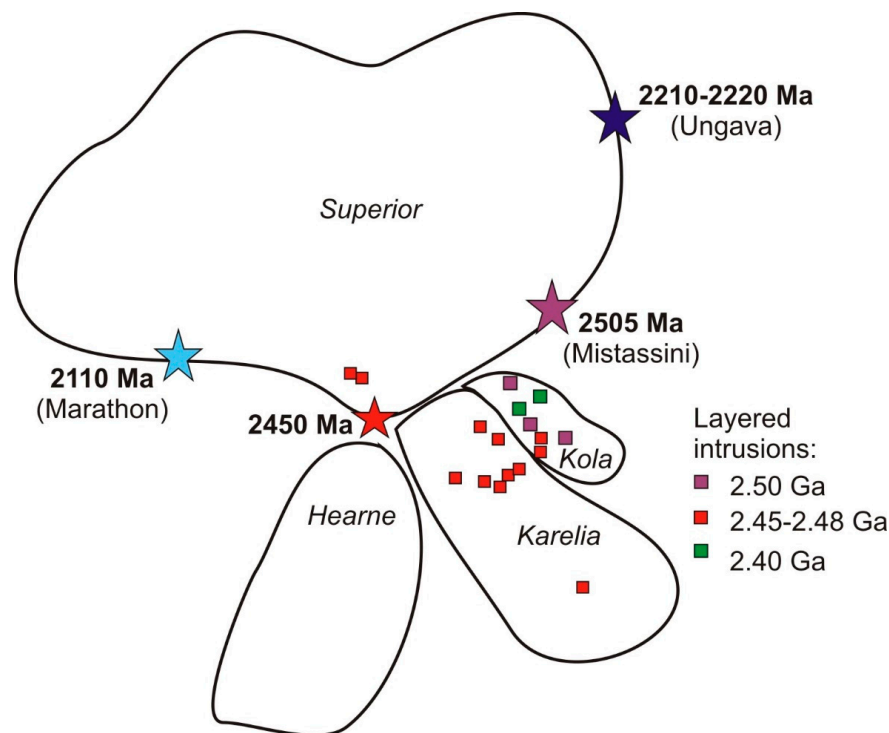


Figure 11. Correlation for the Superior, Karelia and Hearne cratons (based on Reference [72] with amendments).

Author Contributions: Conceptualization, T.B., A.K. and P.S.; Methodology, T.B., A.M., P.S., I.K. and D.E.; Validation, T.B.; Formal Analysis, N.E., E.N. and P.S.; Investigation, T.B., A.M., P.S., N.E., E.N., I.K. and D.E.; Sampling A.K. and M.H.; Writing—Original Draft Preparation, T.B.; Writing—Review & Editing, T.B. and M.H.; Supervision, T.B.

Funding: This research was funded by the Russian Foundation of Basic Researches (RFBR), grant numbers 18-35-00246, 16-05-00305 and 18-05-70082, Program of the Presidium of RAS No. 4.

Acknowledgments: The authors thank their colleagues J. Ludden, F. Corfu, W. Todt, U. Poller, L. Koval, L. Lyalina and N. Levkovich for their kind assistance in conducting the current research. The authors express their special gratitude to T.A. Miroshnichenko and E.N. Steshenko for editing the manuscript and unknown reviewers for their contribution to the improvement of this paper.

Conflicts of Interest: The authors declare no conflict of interest.

References

1. Bogdanova, S.V.; Bingen, B.; Gorbatshev, R.; Kheraskova, T.N.; Kozlov, V.I.; Puchkov, V.N.; Volozh, Y.U. The East European Craton (Baltica) before and during the assembly of Rodinia. *Precambrian Res.* **2008**, *160*, 23–45. [[CrossRef](#)]
2. Slabunov, A.I.; Lobach-Zhuchenko, S.B.; Slabunov, A.I.; Lobach-Zhuchenko, S.B.; Bibikova, E.V.; Sorjonen-Ward, P.; Balagansky, V.V.; Volodichev, O.I.; Shchipansky, A.A.; Svetov, S.A.; et al. The Archaean nucleus of the Fennoscandian (Baltic) Shield. In *European Lithosphere Dynamics*; Gee, D.G., Stephenson, R.A., Eds.; Geological Society: London, UK, 2006; Volume 32, pp. 627–644.
3. Bayanova, T.; Mitrofanov, F.; Serov, P.; Nerovich, L.; Yekimova, N.; Nitkina, E.; Kamensky, I. Layered PGE Paleoproterozoic (LIP) Intrusions in the N-E Part of the Fennoscandian Shield—Isotope Nd-Sr and $^3\text{He}/^4\text{He}$ Data, Summarizing U-Pb Ages (on Baddeleyite and Zircon), Sm-Nd Data (on Rock-Forming and Sulphide Minerals), Duration and Mineralization. In *Geochronology—Methods and Case Studies/Edited by Nils-Axel Mörner*; INTECH: Houston, TX, USA, 2014; pp. 143–193. [[CrossRef](#)]
4. Alapieti, T.T. The Koillismaa layered igneous complex, Finland: Its structure, mineralogy and geochemistry, with emphasis on the distribution of chromium. *Geol. Surv. Finl.* **1982**, *319*, 116.

5. Iljina, M.; Hanski, E. Layered mafic intrusions of the Tornio-Näränkäväära belt. In *Precambrian Geology of Finland—Key to the Evolution of the Fennoscandian Shield*; Lehtinen, M., Nurmi, P.A., Rämö, O.T., Eds.; Elsevier: Amsterdam, The Netherlands, 2005; pp. 101–138.
6. Vogel, D.C.; Vuollo, J.I.; Alapieti, T.T.; James, R.S. Tectonic, stratigraphic and geochemical comparison between ca. 2500–2440 Ma mafic igneous events in the Canadian and Fennoscandian Shields. *Precambrian Res.* **1998**, *92*, 89–116. [[CrossRef](#)]
7. Mitrofanov, F.P.; Balabonin, N.L.; Bayanova, T.B. Main results from the study of the Kola PGE-bearing province, Russia. In *Mineral Deposits*; Papunen, H., Gorbunov, G.I., Eds.; Balkema: Rotterdam, The Netherlands, 1997; pp. 483–486.
8. Ernst, R.E. *Large Igneous Provinces*; Cambridge University Press: Cambridge, UK, 2014; Volume 653.
9. Mitrofanov, F.P.; Korchagin, A.U.; Dudkin, K.O.; Rundkvist, T.V. Fedorovo-Pana layered mafic intrusion (Kola peninsula, Russia): Approaches, methods and criteria for prospecting PGEs. In *Exploration for Platinum-Group Elements Deposits*; Short Course Delivered on Behalf of the Mineralogical Association of Canada in Oulu, Finland; University of Toronto: Toronto, ON, Canada, 2005; Volume 35, pp. 343–358.
10. Schissel, D.; Tsvetkov, A.A.; Mitrofanov, F.P.; Korchagin, A.U. Basal platinum-group element mineralization in the Fedorov Pansky layered mafic intrusion, Kola Peninsula, Russia. *Econ. Geol.* **2002**, *97*, 1657–1677. [[CrossRef](#)]
11. Sharkov, Y.V. *Formation of Layered Intrusions and Related Mineralization*; Scientific World: Moscow, Russia, 2006; p. 364.
12. Bayanova, T.B.; Ludden, J.; Mitrofanov, F.P. Timing and duration of Palaeoproterozoic events producing ore-bearing layered intrusions of the Baltic Shield: Metallogenic, petrological and geodynamic implications. In *Palaeoproterozoic Supercontinents and Global Evolution*; Reddy, S.M., Mazumder, R., Evans, D.A.D., Collins, A.S., Eds.; Geological Society: London, UK, 2009; Volume 323, pp. 165–198.
13. Ekimova, N.A.; Serov, P.A.; Bayanova, T.B.; Elizarova, I.R.; Mitrofanov, F.P. New data on distribution of REEs in sulfide minerals and Sm-Nd dating of ore genesis of layered mafic intrusions. *Dokl. Earth Sci.* **2011**, *436*, 28–31. [[CrossRef](#)]
14. Kullerud, K.; Skjerlie, K.P.; Corfu, F.; De La Rosa, J. The 2.40 Ga Ringvassøy mafic dikes, West Troms Basement Complex, Norway: The concluding act of early Palaeoproterozoic continental breakup. *Precambrian Res.* **2006**, *150*, 183–200. [[CrossRef](#)]
15. Mitrofanov, F.P.; Bayanova, T.B.; Korchagin, A.U.; Groshev, N.Y.; Malitch, K.N.; Zhironov, D.V.; Mitrofanov, A.F. East Scandinavian and Noril'sk plume mafic Large Igneous Provinces of Pd-Pt ores: Geological and metallogenic comparison. *Geol. Ore Depos.* **2013**, *55*, 305–319. [[CrossRef](#)]
16. Balashov, Y.A.; Bayanova, T.B.; Mitrofanov, F.P. Isotope data on the age and genesis of layered mafic-ultramafic intrusions in the Kola Peninsula and northern Karelia, northeastern Baltic Shield. *Precambrian Res.* **1993**, *64*, 197–205. [[CrossRef](#)]
17. Zozulya, D.R.; Bayanova, T.B.; Nelson, E.G. Geology and age of the late Archaean Keivy alkaline province, NE Baltic Shield. *Geology* **2005**, *113*, 601–608. [[CrossRef](#)]
18. Godel, B.; Barnes, S.-J.; Maier, W.-D. Platinum-group elements in sulphide minerals, platinum-group minerals, and whole-rocks of the Merensky Reef (Bushveld Complex, South Africa): Implications for the formation of the reef. *J. Petrol.* **2007**, *48*, 1569–1604. [[CrossRef](#)]
19. Latypov, R.M.; Chistyakova, S.Y. *Mechanism for Differentiation of the Western-Pana Layered Intrusion*; Publ. of KSC RAS: Apatity, Russia, 2000; Volume 315.
20. Balabonin, N.L.; Subbotin, V.V.; Skiba, V.I.; Voitekhovskiy, Y.L.; Savchenko, E.E.; Pakhomovskiy, Y.A. Forms of occurrence and balance of precious metals in the Fedorovo-Pansky intrusion ores (the Kola Peninsula). *Obog. Rud.* **1998**, *6*, 24–30.
21. Subbotin, V.V.; Korchagin, A.U.; Savchenko, E.E. Platinometal mineralization of Fedorovo-Pansky ore region: Type of ore-bearing, mineral composition, particularity of genesis. *Vestn. KSC RAS* **2012**, *1*, 55–65.
22. Krogh, T.E. A low-contamination method for hydro-thermal dissolution of zircon and extraction of U and Pb for isotopic age determinations. *Geochim. Cosmochim. Acta* **1973**, *37*, 485–494. [[CrossRef](#)]
23. Ludwig, K.R. *PBDAT—A Computer Program for Processing Pb-U-Th Isotope Data*; Version 1.22. Open-File Report 88-542; U.S. Geological Survey: Reston, VA, USA, 1991; p. 38.
24. Ludwig, K.R. *ISOPLLOT/Ex—A Geochronological Toolkit for Microsoft Excel*; Version 2.05; Berkeley Geochronology Center Special Publication: Berkeley, CA, USA, 1999; Volume 1a, p. 49.

25. Stacey, J.S.; Kramers, J.D. Approximation of terrestrial lead isotope evolution by a two-stage model. *Earth Planet. Sci. Lett.* **1975**, *26*, 207–221. [[CrossRef](#)]
26. Steiger, R.H.; Jäger, E. Subcommission on Geochronology: Convention on the use of decay constants in geo- and cosmochronology. *Earth Planet. Sci. Lett.* **1977**, *36*, 359–362. [[CrossRef](#)]
27. Jacobsen, S.B.; Wasserburg, G.J. Sm-Nd isotopic evolution of chondrites and achondrites. II. *Earth Planet. Sci. Lett.* **1984**, *67*, 137–150. [[CrossRef](#)]
28. Goldstein, S.J.; Jacobsen, S.B. Nd and Sr isotopic systematics of river water suspended material implications for crystal evolution. *Earth Plan. Sci. Lett.* **1988**, *87*, 249–265. [[CrossRef](#)]
29. Zhuravlyov, A.Z.; Zhuravlyov, D.Z.; Kostitsyn, Y.A.; Chernyshov, I.V. Determination of the Sm-Nd ratio for geochronological purposes. *Geochemistry* **1987**, *8*, 1115–1129.
30. DePaolo, D.J. Neodymium isotopes in the Colorado Front Range and crust-mantle evolution in the Proterozoic. *Nature* **1981**, *291*, 193–196. [[CrossRef](#)]
31. Liew, I.C.; Hofmann, A.W. Precambrian crustal components, plutonic associations, plate environment of the Hercinian Fold Belt of central Europe: Indications from a Nd and Sr isotopic study. *Contrib. Mineral. Petrol.* **1988**, *98*, 129–138. [[CrossRef](#)]
32. Van Achterbergh, E.; Ryan, C.G.; Griffin, W.L. GLITTER: On-line interactive data reduction for the laser ablation ICP-MS microprobe. In Proceedings of the IX V.M. Goldschmidt Conference, Cambridge, MA, USA, 22–27 August 1999; Lunar and Planetary Institute Contribution No. 791: Houston, TX, USA, 1999; Volume 305.
33. Ekimova, N.A.; Serov, P.A.; Bayanova, T.B.; Yelizarova, I.R.; Mitrofanov, F.P. The REE distribution in sulphide minerals and Sm-Nd age determination for the ore-forming processes in mafic layered intrusions. *Dokl. RAS* **2011**, *436*, 75–78.
34. Nitkina, E.A. U-Pb zircon dating of rocks of the platiniferous Fedorova-Pana Layered Massif, Kola Peninsula. *Dokl. Earth Sci.* **2006**, *408*, 551–554. [[CrossRef](#)]
35. Serov, P.A.; Nitkina, E.A.; Bayanova, T.B.; Mitrofanov, F.P. Comparison of the new data on dating using U-Pb and Sm-Nd isotope methods of early barren phase rocks and basal ore-hosting rocks of the Pt-bearing Fedorovo-Pansky layered intrusion (Kola peninsula). *Dokl. Earth Sci.* **2007**, *415*, 1–3.
36. Faure, G. *Principles of Isotope Geology*; Wiley: New York, NY, USA, 1986; Volume 460.
37. Eisele, J.; Sharma, M.; Galer, S.J.G. The role of sediment recycling in EM-1 inferred from Os, Pb, Hf, Nd, Sr isotope and trace element systematic of the Pitcairn Hotspot, *Earth Planet. Sci. Lett.* **2002**, *196*, 197–212. [[CrossRef](#)]
38. Hofmann, A.W. Mantle geochemistry: The message from oceanic volcanism. *Nature* **1997**, *385*, 219–229. [[CrossRef](#)]
39. Yang, S.-H.; Hanski, E.; Li, C.; Maier, W.-D.; Huhma, H.; Mokrushin, A.V.; Latypov, R.; Lahaye, Y.; O'Brien, H.; Qu, W.-J. Mantle source of the 2.44–2.50 Ga mantle plume-related magmatism in the Fennoscandian Shield: Evidence from Os, Nd and Sr isotope compositions of the Monchepluton and Kemi intrusions. *Miner. Depos.* **2016**, *51*, 20. [[CrossRef](#)]
40. Mitrofanov, F.; Golubev, A. Russian Fennoscandian metallogeny. In Proceedings of the Abstracts of the 33 IGC, Oslo, Norway, 6–14 August 2008.
41. Richardson, S.H.; Shirey, S.B. Continental mantle signature of Bushveld magmas and coeval diamonds. *Nature* **2008**, *453*, 910–913. [[CrossRef](#)] [[PubMed](#)]
42. Maier, W.-D.; Halkoaho, T.; Huhma, H.; Hanski, E.; Barnes, S.-J. The Penikat Intrusion, Finland: Geochemistry, geochronology, and origin of platinum-palladium reefs. *J. Petrol.* **2018**, *59*, 967–1006. [[CrossRef](#)]
43. Perttunen, V.; Vaasjoki, M. U-Pb geochronology of the Peräpohja Schist Belt, northwestern Finland. In *Radiometric Age Determinations from Finnish Lapland and Their Bearing on the Timing of Precambrian Volcano-Sedimentary Sequences*; Vaasjoki, M., Ed.; Special Paper 33; Geological Survey of Finland: Espoo, Finland, 2001; pp. 45–84.
44. Mitrofanov, F.P.; Bayanova, T.B. Duration and timing of ore-bearing Palaeoproterozoic intrusions of Kola province. In *Mineral Deposits: Processes to Processing*; Stanley, C.J., Ed.; Balkema: Rotterdam, The Netherlands, 2002; pp. 1275–1278.
45. Amelin, Y.V.; Heaman, L.M.; Semenov, V.S. U-Pb geochronology of layered mafic intrusions in the eastern Baltic Shield: Implications for the timing and duration of Palaeoproterozoic continental rifting. *Precambrian Res.* **1995**, *75*, 31–46. [[CrossRef](#)]

46. Kramm, U. Mantle components of carbonatites from the Kola Alkaline Province, Russia and Finland: A Nd-Sr study. *Eur. J. Mineral.* **1993**, *5*, 985–989. [[CrossRef](#)]
47. Heaman, L.M.; Le Cheminant, A.N. Paragenesis and U-Pb systematics of baddeleyite (ZrO). *Chem. Geol.* **1993**, *110*, 95–126. [[CrossRef](#)]
48. Fischer-Godde, M.; Becker, H.; Wombacher, F. Rhodium, gold and other highly siderophile element abundances in chondritic meteorites. *Geochim. Cosmochim. Acta* **2010**, *74*, 356–379. [[CrossRef](#)]
49. Lyubetskaya, T.; Korenaga, J. Chemical composition of Earth's primitive mantle and its variance: 2. Implications for global geodynamics. *J. Geophys. Res.* **2007**, *112*. [[CrossRef](#)]
50. Lyubetskaya, T.; Korenaga, J. Chemical composition of Earth's primitive mantle and its variance: 1. Method and results. *J. Geophys. Res.* **2007**, *112*. [[CrossRef](#)]
51. Amelin, Y.V.; Semenov, V.S. U-Nd and Sr isotopic deochemistry of mafic layered intrusions in the eastern Baltic Shield: Implications for the evolution of Paleoproterozoic continental mafic magmas. *Contrib. Mineral. Petrol.* **1996**, *124*, 255–272. [[CrossRef](#)]
52. Bayanova, T.B.; Smolkin, V.F.; Levkovich, N.V. U-Pb geochronological study of Mount Generalskaya layered intrusion, northwestern Kola Peninsula, Russia. In *Transactions of the Institution of Mining and Metallurgy; Institution of Mining and Metallurgy: Vladikavkaz, Russia, 1999; Volume 108*, pp. B83–B90.
53. Tolstikhin, I.N.; Dokuchaeva, V.S.; Kamensky, I.L.; Amelin, Y.V. Juvenile helium in ancient rocks: II. U-He, K-Ar, Sm-Nd, and Rb-Sr systematics in the Monchepluton. $^3\text{He}/^4\text{He}$ ratios frozen in uranium-free ultramafic rocks. *Geochim. Cosmochim. Acta* **1992**, *56*, 987–999. [[CrossRef](#)]
54. Vrevsky, A.B.; Levchenkov, O.A. Geological-geochronological scale of the endogenous processes operated within the Precambrian complexes of the central part of the Kola Peninsula. In *Geodynamics and Deep Structure of the Soviet Baltic Shield*; Mitrofanov, F.P., Bolotov, V.I., Eds.; KSC RAS: Apatity, Russia, 1992; Volume 150.
55. Mitrofanov, F.P.; Balagansky, V.V.; Balashov, Y.A.; Gannibal, L.F.; Dokuchaeva, V.S.; Nerovich, L.I.; Radchenko, M.K.; Ryungenen, G.I. U-Pb age for gabbro-anorthosite of the Kola Peninsula. *Dokl. RAS* **1993**, *331*, 95–98.
56. Bayanova, T.B. Baddeleyite: A promising geochronometer for alkaline and basic magmatism. *Petrology* **2006**, *14*, 187–200. [[CrossRef](#)]
57. Huhma, H.; Cliff, R.; Perttunen, V.; Sakko, M. Sm-Nd and Pb isotopic study of mafic rocks associated with early Proterozoic continental rifting: The Perapohja schist belt in northern Finland. *Contrib. Mineral. Petrol.* **1990**, *104*, 369–379. [[CrossRef](#)]
58. Alapieti, T.T.; Filen, B.A.; Lahtinen, J.J.; Lavrov, M.M.; Smolkin, V.F.; Voitekhovsky, Y.L. Early Proterozoic layered intrusions in the Northeastern part of the Fennoscandian Shield. *Contrib. Mineral. Petrol.* **1990**, *42*, 1–22. [[CrossRef](#)]
59. Hanski, E.; Walker, R.J.; Huhma, H.; Suominen, I. The Os and Nd isotopic systematics of c. 2.44 Ga Akanvaara and Koitelainen mafic layered intrusions in northern Finland. *Precambrian Res.* **2001**, *109*, 73–102. [[CrossRef](#)]
60. Bayanova, T.B.; Mitrofanov, F.P. Layered Proterozoic PGE intrusions in Kola region: New isotope data. In *Proceedings of the Extended abstracts of the X International Symp. Platinum "Platinum-Group Elements—From Genesis to Beneficiation and Environmental Impact"*, Oulu, Finland, 8–11 August 2005; pp. 289–291.
61. Nerovich, L.I.; Bayanova, T.B.; Serov, P.A.; Elizarov, D.V. Magmatic sources of dikes and veins in the Moncha Tundra Massif, Baltic Shield: Isotopic-geochronologic and geochemical evidence. *Geochem. Intern.* **2014**, *52*, 548–566. [[CrossRef](#)]
62. Rundkist, T.V.; Bayanova, T.B.; Sergeev, S.A.; Pripachkin, P.V.; Grebnev, P.A. The Paleoproterozoic Vurechuaivench layered Pt-bearing pluton, Kola Peninsula: New results of the U-Pb (ID-TIMS, SHRIMP) dating of baddeleyite and zircon. *Dokl. Earth Sci.* **2014**, *454*, 1–6. [[CrossRef](#)]
63. Mitrofanov, F.P.; Bayanova, T.B.; Zhiron, D.V.; Serov, P.A.; Golubev, A. Geological and isotope-geochemical characteristics of prediction and search method for the PGE-bearing mafic-ultramafic layered intrusions of the East-Scandinavian LIP. In *Proceedings of the Abstracts of the XII Intern. Platinum Symp.*, Yekaterinburg, Russia, 11–14 August 2014; pp. 113–114.
64. Chistyakov, A.V.; Bogatkov, O.A.; Grochovskaya, T.L.; Sharkov, E.V.; Belyatskiy, B.V.; Ovchinnikova, G.V. Burakovskiy layered pluton (S. Karelia) as a result of space combination double intrusive bodies: Petrological and isotope-geochemical data. *Dokl. RAS* **2000**, *372*, 228–235.
65. Gorbatshev, R.; Bogdanova, S. Frontiers in the Baltic Shield. *Precambrian Res.* **1993**, *64*, 3–21. [[CrossRef](#)]

66. Vuollo, J.I.; Huhma, H. Palaeoproterozoic mafic dikes in NE Finland. In *Precambrian Geology of Finland*; Lehtinen, M., Nurmi, P.A., Rämö, O.T., Eds.; Elsevier: Amsterdam, The Netherlands, 2005; pp. 195–236.
67. Vuollo, J.I.; Huhma, H.; Stepana, V.; Fedotov, G.A. Geochemistry and Sm-Nd isotope studies of a 2.45 Ga dike swarm: Hints at parental magma compositions and PGE potential to Fennoscandian layered intrusions. In *Proceedings of the IX Intern. Platinum Symp.*, Billings, MT, USA, 21–25 July 2002; pp. 469–470.
68. Coffin, M.F.; Eldholm, O. Large igneous provinces: Crustal structure, dimensions and external consequences. *Rev. Geophys.* **1994**, *32*, 1–36. [[CrossRef](#)]
69. Ernst, R.E.; Buchan, K.L. Recognizing mantle plumes in the Geological Record. *Earth Planet. Sci.* **2003**, *31*, 469–523. [[CrossRef](#)]
70. Pirajno, F. Mantle plumes, associated intraplate tectono-magmatic processes and ore systems. *Episodes* **2007**, *30*, 6–19.
71. Tolstikhin, I.N.; Marty, B. The evolution of terrestrial volatiles: A view from helium, neon, argon and nitrogen isotope modeling. *Chem. Geol.* **1998**, *147*, 27–52. [[CrossRef](#)]
72. Bleeker, W.; Ernst, R. Short-lived mantle generated magmatic events and their dike swarms: The key unlocking Earth's Paleogeographic record back to 2.6 Ga. In *Dike Swarms-Time Marker of Crustal Evolution*; Balkema Publishers: Zürich, Switzerland, 2006; pp. 1–20.
73. Campbell, I.H. Identification of ancient mantle plumes. In *Mantle Plumes: Their Identification Through Time*; Ernst, R.E., Buchan, K.L., Eds.; Geological Society of America: Boulder, CO, USA, 2001; Volume 352, pp. 5–22.
74. Heaman, L.M. Global mafic magmatism at 2.45 Ga: Remnants of an ancient large igneous province? *Geology* **1997**, *25*, 299–302. [[CrossRef](#)]
75. Bogatikov, O.A.; Kovalenko, V.I.; Sharkov, Y.V. *Magmatism, Tectonics, and Geodynamics of the Earth*; Nauka: Moscow, Russia, 2010; 606p.
76. Grachyov, A.F. Identification of mantle plumes on the basis of studying composition and isotope geochemistry of volcanic rocks. *Petrology* **2003**, *11*, 618–654.



© 2019 by the authors. Licensee MDPI, Basel, Switzerland. This article is an open access article distributed under the terms and conditions of the Creative Commons Attribution (CC BY) license (<http://creativecommons.org/licenses/by/4.0/>).